JOURNAL OF VIROLOGY, July 2009, p. 6917–6921 Vol. 83, No. 13
0022-538X/09/$08.00+0 doi:10.1128/JVI.00081-09

NOTES

Enumeration of an Extremely High Particle-to-PFU Ratio for Varicella-Zoster Virus▽†

John E. Carpenter, Ernesto P. Henderson, and Charles Grose*

Central Microscopy Research Facility, University of Iowa, Iowa City, Iowa 52242

Received 13 January 2009/Accepted 9 April 2009

Varicella-zoster virus (VZV) is renowned for its low titers. Yet investigations to explore the low infectivity are hampered by the fact that the VZV particle-to-PFU ratio has never been determined with precision. Herein, we accomplish that task by applying newer imaging technology. More than 300 images were taken of VZV-infected cells on 4 different samples at high magnification. We enumerated the total number of viral particles within 25 cm^2 of the infected monolayer at 415 million. Based on these numbers, the VZV particle:PFU ratio was approximately 40,000:1 for a cell-free inoculum.

A precise ratio of particles to PFU of varicella-zoster virus (VZV) has never been determined, even though VZV was first isolated in cell culture by the Nobel laureate T. H. Weller in 1952 (21). His group determined that VZV replicated in a few embryonic tissues and in amnion cells. Subsequently, Taylor-Robinson and Caunt found that VZV replication was restricted to a small number of mainly embryonic cells by testing more than 20 primary and continuous cell lines (19). A decade later, VZV was propagated in melanoma cell lines, which are derived from the neural crest (8). In all of these cultured cells, the titer was found to be low, particularly when compared with that of the closely related herpes simplex type 1 virus (HSV-1). Again, in sharp contrast with HSV-1, the virus remained strongly cell associated.

The term particle/PFU ratio refers to the number of viral particles required to form one plaque in a plaque assay. It is a measure of the efficiency by which a virus infects cultured cells. Early in the 1960s, investigators began using negative staining electron microscopy to count viral particles in inoculum material and compare those counts to the measured titer, thereby measuring ratios for a few animal viruses (6). For example, the ratio for HSV-1 is around 10:1 (10, 20). Due to the strong cell association of VZV infection of cultured cells, no precise VZV particle/PFU ratio has ever been determined. The lack of any widely accepted VZV ratio severely limits our ability to assess whether mutated or recombinant viruses produce more or fewer complete infectious particles in cultured cells (4, 5, 15, 17). In other words, if an attenuated virus has a lower titer, we do not know whether fewer viral particles are produced per square centimeter of cellular monolayer (without a change in the particle/PFU ratio) or alternatively fewer infectious viral particles are produced overall (with a higher particle/PFU ratio).

In this report, we successfully define a VZV particle/PFU ratio by imaging viral particles with advanced scanning electron microscopic (SEM) technology not available during our earlier investigations of viral structure (12). We demonstrate that the VZV ratio is much higher than that for other common human viruses grown in cultured cells and remarkably higher than that for HSV. Finally, this report documents evidence of an ever-widening difference between HSV and VZV replication and assembly in cultured cells (7, 13, 18).

Topography of viral particles on infected cell surface. In a recent study, we used newer imaging technology to document that a vast majority of VZV particles were noninfectious envelopes lacking a capsid (3, 14, 16). Because of those results, we postulated that obtaining a particle/PFU ratio would provide valuable insight into continuing investigations to explain low VZV infectivity. In an effort to better understand what is meant by cell-free virus, we repeated experiments first conducted decades ago by ourselves and others. The standard protocol stipulated dislodging infected cells with a rubber policeman. After sonication of the cell pellet, titers of cell-free virus around 10,000 PFU/25 cm^2 monolayer were obtained. In an alternative protocol, we substituted trypsin dispersion of an infected monolayer, followed by washing to remove the trypsin. When we subsequently sonicated the pellet of trypsin-dispersed cells, we obtained little or no infectious cell-free virus (<100 PFU/25 sq cm). Our results confirmed an earlier, similar result reported by Brunell (2). From these results, we surmised that cell-free virus consisted of virus that had entered the outer cell membrane, only to be separated from the membrane by sonication. Trypsin treatment presumably removed or destroyed this virus. We had previously demonstrated that infectious virus is easily disassociated from an infected cell monolayer. Based on these cumulative observations, we decided to enumerate the viral particles detectable in the outer cell membrane of infected cells (Fig. 1). We postulated that by counting

* Corresponding author. Mailing address: University of Iowa Hospital, 200 Hawkins Drive, Iowa City, IA 52242. Phone: (319) 356-2270. Fax: (319) 356-4855. E-mail: charles-grose@uiowa.edu.

† Supplemental material for this article may be found at http://jvi.asm.org/.

▽ Published ahead of print on 15 April 2009.

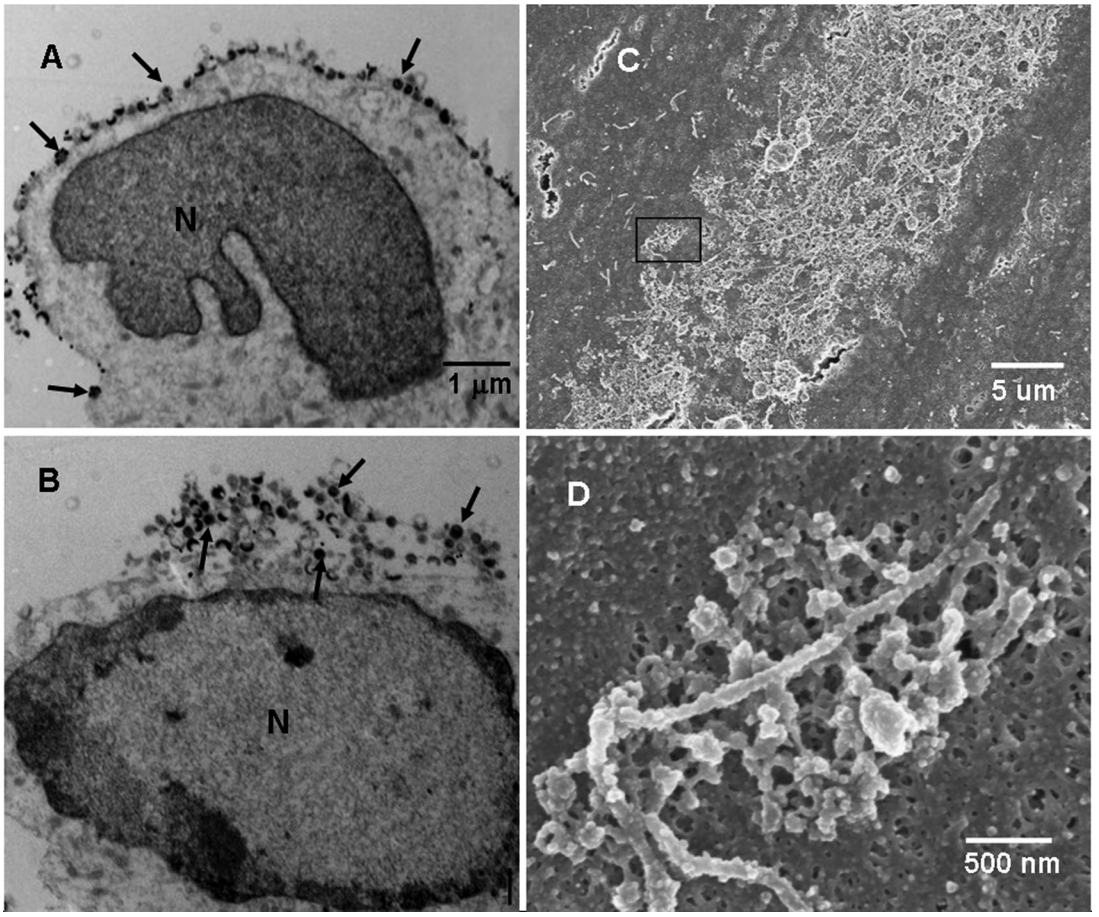

FIG. 1. Potential cell-free VZV on the surfaces of infected cells. Melanoma cells were inoculated with VZV-32-infected cells (1:8), fixed at 72 h postinfection, and then processed for viewing in transmission and scanning electron microscopes. Representative transmission electron microscopy sections (A and B) through VZV-infected cells showed the majority of VZV particles are on or near the surface of the infected cell rather than in the cytoplasm. Particles with discernible cores (capsid and DNA) are marked by black arrows. (C) SEM image of a section of a viral highway at magnification ×3,500. Small viral particles were clustered within the highway. (D) Image at magnification ×35,000 of the area enclosed by the rectangle in panel C. The image shows a single cluster of viral particles arranged along a filopodium. The majority of the visible particles were aberrant. N, nucleus.

these surface particles, we would obtain a denominator for the total number of potentially infectious VZV particles.

VZV particles egress across the infected cell syncytia in long pathways that were called viral highways by Harson and Grose (12). More recently, examination of VZV viral highways by a newer generation of SEM documented that the highways were composed of both complete and incomplete or aberrant viral particles (which we called VZV L particles) clustered at the base of filopodia (3). VZV highways ranged in width from 10 to 50 μm and in length from 30 to 300 μm (Fig. 1C). Viral particles egressed in clumps of 5 to 10 viral particles clustered around several interconnected filopodia (Fig. 1D).

Measurement of viral particle density. We performed an experiment to choose a magnification that balances between being low enough to accurately calculate the particle density and high enough to clearly see whether a particle was complete or not. We found that the error in computing viral density increased slowly past magnification ×40,000 and became inaccurate at magnification ×80,000; therefore, we chose to randomly sample highways at ×35,000. The only constraints were that the image had to be within a viral highway and that at least one viral particle was visible. Additionally, enumerated viral particles were classified as complete or L particles. An L particle is characterized by the lack of a capsid, which is apparent in large gaps in the viral particle structure. Complete particles are those that contain no large gaps and are spherical and covered with protuberances.

In an earlier report (3), we established that both aberrant and complete particles were detected on the cell surface. In this investigation, we further defined the proportions of these groups of particles. Using four different samples of melanoma cells infected with VZV-32 for 72 h postinfection, we obtained 303 images at magnification ×35,000 of different aspects of viral highways on the surfaces of the infected cells. Two images from that set are shown in Fig. 2A and B. Image A contained 26 viral particles of which only 6 were complete, while Image B contained 29 viral particles of which 4 were complete. The resulting viral particle densities were 2.93 and 3.27 particles/μm^2, respectively. The percentages of complete particles were 6/26 (23.1%) and 4/29 (13.8%).

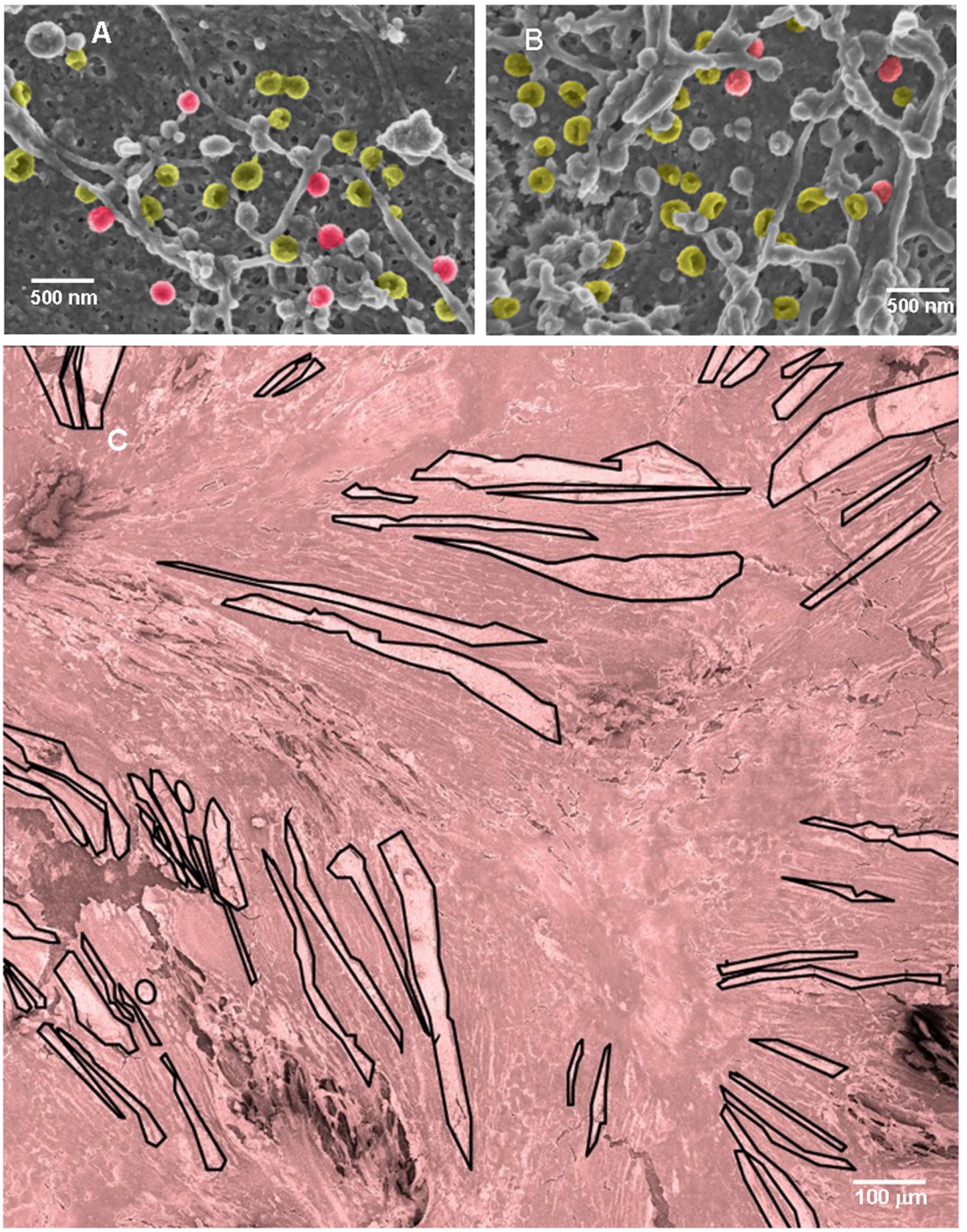

FIG. 2. Representative SEM images from the set used to estimate the number of viral particles on infected cells. (A and B) Two images that are representative of 303 SEM images at magnification ×35,000, taken of various sections of viral highways in four different samples. Panel A contains 26 particles: 6 are complete; 20 are L particles. Panel B contains 29 particles: 4 are complete; 25 are L particles. The density of viral particles in panels A and B was 2.9 and 3.3 particles/μm^2, respectively. L particles are pseudocolored yellow; complete particles are red. (C) Forty-eight overlapping images of three different areas of each sample were taken at magnification ×600 and then pieced together to make 12 individual montages that each show approximately 1 mm^2 of infected cell surface. One of the montages (S1-A) is shown, with all viral highways measured in this study outlined in black. It is pseudocolored red. Full-size versions of all 12 montages are available in the supplemental material.

Distributions of viral particle density and percentage of complete particles. The distribution of calculated viral particle densities over images was generated by binning each image by its density in increments of 0.5 (Fig. 3). Similarly, the distribution of percentages of complete particles was generated by binning each image by its percentage of complete particles in increments of 10.0 (Fig. 3). The density distributions from all four samples exhibited a positively skewed normal curve with a

A	S1	S2	S3	S4	All
Number of images	71	82	75	75	303
Average particle density (/μm²)	1.9	1.5	1.4	2.8	2.0
SD of particle density (/μm²)	0.8	0.7	0.7	1.1	1.0
Average % of complete particles	19.2	14.8	13.2	14.0	15.2
SD of % of complete particles	10.8	10.2	11.2	7.8	10.3

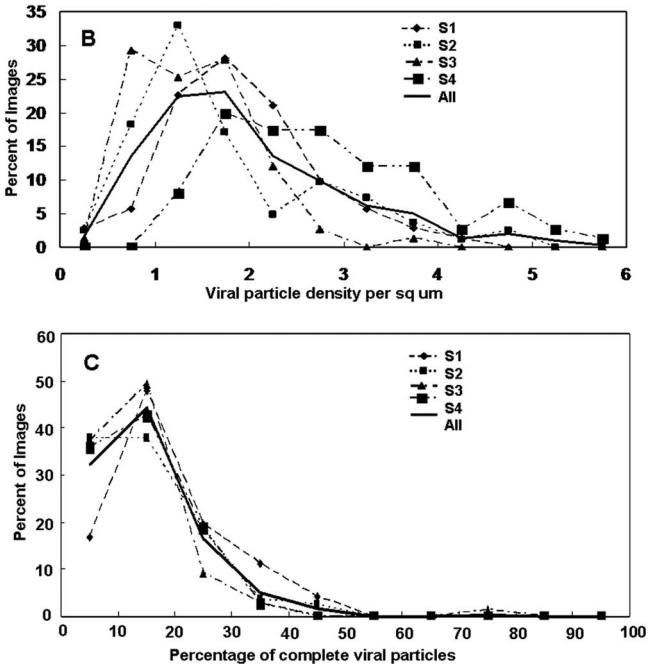

FIG. 3. Density and composition of viral particles on VZV-infected cells. (A) Statistical analysis of viral particle density and composition for all four samples. (B) Percentage of images that had a particular viral particle density for all four samples separately and then all images grouped together. The graph shows skewed normal distributions centered around 1.8 particles/μm^2 with a range up to 4.0. The distribution was similar for all four samples. (C) Percentage of images that had a particular percentage of complete particles. The graph also shows a skewed normal distribution centered around 15% complete particles, with a range up to 40% complete particles.

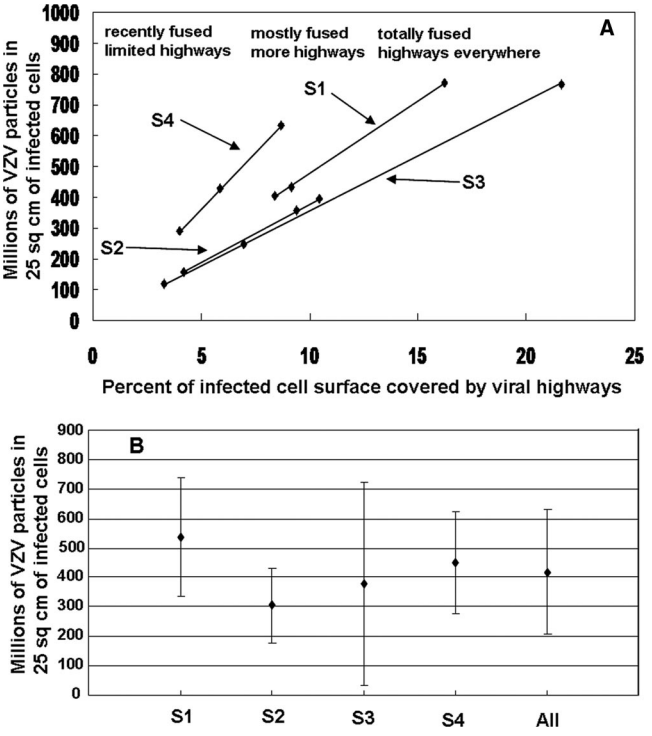

FIG. 4. Enumeration of VZV particles in 25 cm^2 of infected cells. Measurements of viral highways in 12 montages of infected cells (Fig. 2C; see also the supplemental material) were used to determine the area of infected cell surface covered by viral highways in each montage. Multiplying the area by the viral particle density calculated for each sample yielded an estimate for the total number of VZV particles in 25 cm^2. (A) Graph of estimated particle numbers versus percentage of area covered by viral highways. The slope of each line in the graph corresponds to the viral particle density of the sample. The data points showed the considerable variability of viral egress in individual mm^2 of infected cell surface. (B) Graph of average particle number versus sample. The data points for each sample were derived by averaging the three measurements for each sample. The All data point was the result of averaging all 12 measurements. The error bars correspond to standard deviations. The average number of VZV particles in 25 cm^2 was 415 million ± 200 million.

maximum between 1 and 3 particles/μm^2 and ranging out to 4 or 5 particles/μm^2 (1). The percentage-complete distributions were also skewed normal but more sharp, with a maximum between 10 and 20% and ranging out to 40%. In all images, more than half of all particles were aberrant. The average particle density ranged from 1.4 to 2.8 particles/μm^2, with an overall average of 2.0 ± 1.0 particles/μm^2 (Fig. 3). Correspondingly, the average percentage of complete particles ranged from 13.2% to 19.2%, with an overall overage of 15.2% ± 10.3%, which indicates a preponderance of VZV L particles in viral highways.

Enumeration of viral particles on the surface of an infected monolayer. In order to estimate the total number of viral particles in an infected cell monolayer, we measured the area of the infected cell surface covered by viral highways on three different areas on each of four samples. We accomplished this task by taking an overlapping set of SEM images at magnification ×600 that covered approximately 1 mm^2 of infected cell surface. The overlapping images were then used to generate composite images of the areas (Fig. 2C; see also the supplemental material). Using a large format (30 by 40 cm) on paper, the highways of viral particles were then enumerated and measured with a ruler. For example, the montage in Fig. 2C exhibited 58 highways that covered 8.4% of the area of the montage, while those of montage B of sample S2 and montage C of sample S3 exhibited 74 and 105 highways and covered 10.5% and 21.6% of the montages, respectively. Multiplying the area of all highways in each montage by the corresponding viral particle density led to 12 estimates of the number of viral particles on the infected cell surface (Fig. 4A).

Averaging computed particle numbers for each of the four samples yielded values that ranged from 300 million to 540 million (Fig. 4B). Averaging the computed results for all 12 montages (3 montages × 4 samples) yielded a final number of 415 million VZV particles per 25 cm^2. A typical measured titer for a cell-free VZV infection is 10,000 PFU per 25 cm^2 of infected cells (9, 11).

Conclusion. Taken together, the calculations from this imaging analysis indicated that approximately 40,000 VZV particles in a cell-free inoculum were needed to generate 1 PFU. Of equal interest, our calculations also show that VZV when grown in cultured cells had a higher particle/PFU ratio than any other studied virus (6).

The research was supported in part by NIH grant AI22795. E.P.H. received a stipend from the Iowa Biosciences Advantage Program, funded by NIH NIGMS grant 58939.

REFERENCES

1. **Anderson, D., D. Sweeney, and T. Williams.** 1986. Statistics: concepts and applications. West Publishing Company, St. Paul, MN.
2. **Brunell, P. A.** 1967. Separation of infectious varicella-zoster virus from human embryonic lung fibroblasts. Virology **31:**732–734.
3. **Carpenter, J. E., J. A. Hutchinson, W. Jackson, and C. Grose.** 2008. Egress of light particles among filopodia on the surface of Varicella-Zoster virus-infected cells. J. Virol. **82:**2821–2835.
4. **Cohen, J. I.** 2001. Mutagenesis of the varicella-zoster virus genome: lessons learned. Arch. Virol. **2001** (Suppl.)**:**91–97.
5. **Cohen, J. I., and K. E. Siedel.** 1993. Generation of varicella-zoster virus (VZV) and viral mutants from cosmid DNAs: VZV thymidylate synthetase is not essential for replication in vitro. Proc. Natl. Acad. Sci. USA **90:**7376–7380.
6. **Flint, S. J., L. W. Enquist, V. R. Racaniello, and A. M. Skalka.** 2008. Principles of virology, 3rd ed. ASM Press, Washington, DC.
7. **Granzow, H., B. G. Klupp, W. Fuchs, J. Veits, N. Osterrieder, and T. C. Mettenleiter.** 2001. Egress of alphaherpesviruses: comparative ultrastructural study. J. Virol. **75:**3675–3684.
8. **Grose, C., and P. A. Brunell.** 1978. Varicella-zoster virus: isolation and propagation in human melanoma cells at 36 and 32 degrees C. Infect. Immun. **19:**199–203.
9. **Grose, C., D. M. Perrotta, P. A. Brunell, and G. C. Smith.** 1979. Cell-free varicella-zoster virus in cultured human melanoma cells. J. Gen. Virol. **43:** 15–27.
10. **Harland, J., and S. M. Brown.** 1998. HSV growth, preparation and assay, p. 1–4. *In* S. M. Brown and A. R. MacLean (ed.), Methods in molecular medicine: herpes simplex virus protocols, vol. 10. Humana Press, Totowa, NJ.
11. **Harper, D. R., N. Mathieu, and J. Mullarkey.** 1998. High-titre, cryostable cell-free varicella zoster virus. Arch. Virol. **143:**1163–1170.
12. **Harson, R., and C. Grose.** 1995. Egress of varicella-zoster virus from the melanoma cell: a tropism for the melanocyte. J. Virol. **69:**4994–5010.
13. **Honess, R. W., and B. Roizman.** 1974. Regulation of herpesvirus macromolecular synthesis. I. Cascade regulation of the synthesis of three groups of viral proteins. J. Virol. **14:**8–19.
14. **McLauchlan, J., and F. J. Rixon.** 1992. Characterization of enveloped tegument structures (L particles) produced by alphaherpesviruses: integrity of the tegument does not depend on the presence of capsid or envelope. J. Gen. Virol. **73:**269–276.
15. **Moffat, J. F., L. Zerboni, P. R. Kinchington, C. Grose, H. Kaneshima, and A. M. Arvin.** 1998. Attenuation of the vaccine Oka strain of varicella-zoster virus and role of glycoprotein C in alphaherpesvirus virulence demonstrated in the SCID-hu mouse. J. Virol. **72:**965–974.
16. **Rixon, F. J., C. Addison, and J. McLauchlan.** 1992. Assembly of enveloped tegument structures (L particles) can occur independently of virion maturation in herpes simplex virus type 1-infected cells. J. Gen. Virol. **73:**277–284.
17. **Santos, R. A., C. C. Hatfield, N. L. Cole, J. A. Padilla, J. F. Moffat, A. M. Arvin, W. T. Ruyechan, J. Hay, and C. Grose.** 2000. Varicella-zoster virus gE escape mutant VZV-MSP exhibits an accelerated cell-to-cell spread phenotype in both infected cell cultures and SCID-hu mice. Virology **275:**306–317.
18. **Storlie, J., J. E. Carpenter, W. Jackson, and C. Grose.** 2008. Discordant varicella-zoster virus glycoprotein C expression and localization between cultured cells and human skin vesicles. Virology *38***2:**171–181.
19. **Taylor-Robinson, D., and A. E. Caunt.** 1964. Cell-free varicella-zoster virus in tissue culture. J. Hyg. **62:**413–424.
20. **Watson, D. H., W. C. Russell, and P. Wildy.** 1963. Electron microscopic particle counts on herpes virus using the phosphotungstate negative staining technique. Virology **19:**250–260.
21. **Weller, T. H., and M. B. Stoddard.** 1952. Intranuclear inclusion bodies in cultures of human tissue inoculated with varicella vesicle fluid. J. Immunol. **68:**311–319.